MATERIALS SCIENCE

Writing in the granular gel medium

10.1126/sciadv.1500655

Tapomoy Bhattacharjee,[1] Steven M. Zehnder,[1] Kyle G. Rowe,[1] Suhani Jain,[2] Ryan M. Nixon,[1] W. Gregory Sawyer,[1,3] Thomas E. Angelini[1,4,5]*

Gels made from soft microscale particles smoothly transition between the fluid and solid states, making them an ideal medium in which to create macroscopic structures with microscopic precision. While tracing out spatial paths with an injection tip, the granular gel fluidizes at the point of injection and then rapidly solidifies, trapping injected material in place. This physical approach to creating three-dimensional (3D) structures negates the effects of surface tension, gravity, and particle diffusion, allowing a limitless breadth of materials to be written. With this method, we used silicones, hydrogels, colloids, and living cells to create complex large aspect ratio 3D objects, thin closed shells, and hierarchically branched tubular networks. We crosslinked polymeric materials and removed them from the granular gel, whereas uncrosslinked particulate systems were left supported within the medium for long times. This approach can be immediately used in diverse areas, contributing to tissue engineering, flexible electronics, particle engineering, smart materials, and encapsulation technologies.

Soft granular gel made from polymeric microparticles appears to be a perfect medium in which to write three-dimensional (3D) structures of truly arbitrary design (*1*–*3*). These structures are made by carefully tracing out a series of programmed paths within a granular gel, using a fine hollow tip that fluidizes the medium at the point of injection of the desired material. The rapid solidification of the granular gel then traps and holds the injected material behind the moving tip. Holding material within the jammed medium negates the effects of surface tension, gravity, and particle diffusion, and enables a wide variety of materials to be written by this process, including silicones, hydrogels, colloids, and living cells. Yielding and fluidization in granular matter is known as the jamming/unjamming transition and is a vibrant area of study within the rheology and soft matter communities (*4*–*11*). By placing materials within a jammed soft granular gel medium, the manufacturing of finely detailed delicate materials with nearly limitless aspect ratios is possible. However, the precision and level of detail achieved by writing within a soft granular gel medium may be limited by the size of the granules, which must be larger than 1 μm to eliminate colloidal scale diffusion (*12*–*14*). Functional structures made from soft polymeric materials can be manufactured and removed from the granular gel medium by crosslinking these materials during or after writing. By contrast, uncrosslinked particulate systems such as colloids and cells can be left supported within the medium for long times. To illustrate the precision, ease, and flexibility of this method, we have produced a wide variety of functional structures including complex large aspect ratio 3D objects, thin closed shells, and hierarchically branched vessel networks. This approach can be applied with minimal technical barriers in a diversity of areas, potentially contributing to research in the engineering of tissue and organs, flexible electronics, particle engineering, smart materials, and encapsulation technologies.

One of the most confounding problems in condensed matter physics is the transition between the fluid and disordered solid states (*8*, *15*). Recently, a new complexity has been added to these studies by replacing the traditionally hard particles with soft microscale hydrogel particles (*1*, *10*). Jamming transitions in soft granular gels are graceful and exhibit a smooth variation in material properties when crossing between the fluid and solid states. We leverage this intriguing behavior at the transition to write sophisticated multidimensional structures in a soft granular gel made from 7-μm-diameter hydrogel particles. This medium is fluidized under low shear stresses (1 to 200 Pa), permitting easy insertion and rapid motion of delicate needles deep within the bulk. The locally fluidized gel rapidly resolidifies in the wake to give a permanent and continuous medium that firmly holds the injected material in place (Fig. 1, fig. S1 to S5, and movies S1 and S2).

Three-dimensional printing is usually a race against instabilities; the challenge is to prevent printed material from changing shape after placement (*16*–*19*). Two nearly ubiquitous sources of instability are surface tension, which drives high aspect ratio shapes toward spheres, and body forces, which cause gravity-driven sag and buckling. Minimizing these effects requires clever design of feature spacing and support material layout, and compromises in both materials and processing methods. Writing into viscoelastic materials often requires the rheological optimization of support material, printed material, and a third material that fills in crevasses that are created while writing (*20*, *21*). By contrast, structures can be written into granular gels of widely varying composition without the addition of filler fluids because potential crevasses will spontaneously collapse when the hydrostatic stress at the bottom of the crevasse (ρgh, where ρ is density, g is gravity, and h is depth) exceeds the gel's yield stress (σ_y); a simple dimensionless group predicts collapse if $\sigma_y/(\rho gh) < 1$. Viscous stresses resulting from the viscosity (η) and shear rate (v/d, where v is tip speed and d is diameter) can also be normalized by the hydrostatic stress, and a similar dimensionless ratio predicts the dynamic reflow of fluid into the trailing space if $(v/d)\eta/(\rho gh) < 1$. The granular gel medium described here, composed of Carbopol microgels, satisfies these criteria over a wide concentration range with exceedingly low yield stress and viscosity, the ability to remain solid at extremely low concentrations, and granular characteristics permitting recoverable yielding (see Materials and Methods and fig. S5).

To explore the stability of writing in granular gels, we have generated several complex structures that would otherwise disperse, sag, or fall apart. For example, we created a 4-cm-long model of DNA by arranging long thread-like features about 100 μm in diameter made entirely from uncrosslinked 1-μm fluorescent polystyrene microspheres (0.1%, w/w). While creating these complex 3D structures, the tip writes

[1]Department of Mechanical and Aerospace Engineering, University of Florida, Gainesville, FL 32611, USA. [2]Stanton College Preparatory, Jacksonville, FL 32209, USA. [3]Department of Materials Science and Engineering, University of Florida, Gainesville, FL 32611, USA. [4]J. Crayton Pruitt Family Department of Biomedical Engineering, University of Florida, Gainesville, FL 32611, USA. [5]Institute for Cell and Regenerative Medicine, University of Florida, Gainesville, FL 32611, USA.
*Corresponding author. E-mail: t.e.angelini@ufl.edu

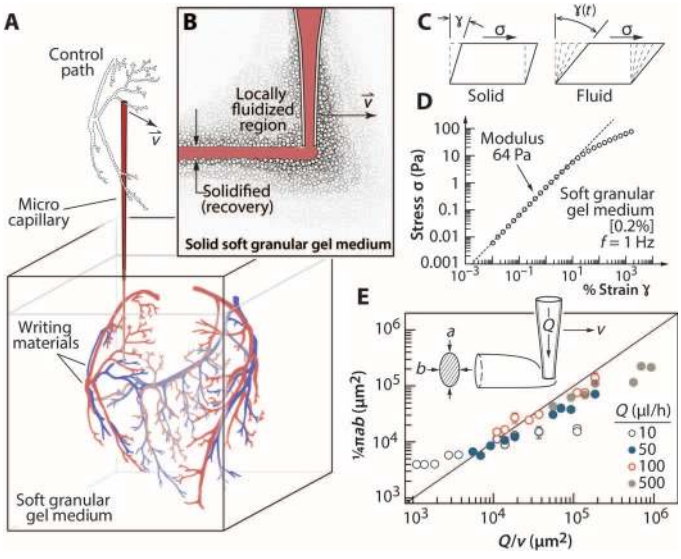

Fig. 1. Granular gel as a 3D writing medium. (**A**) A microscale capillary tip sweeps out a complex pattern as material is injected into the granular gel medium. Complex objects can be generated because the drawn structure does not need to solidify or generate support on its own. (**B**) As the tip moves, the granular gel locally fluidizes and then rapidly solidifies, leaving a drawn cylinder in its wake. The reversible transition allows the tip to traverse the same regions repeatedly. (**C**) The soft granular gel is a yield stress material, which elastically deforms at low shear strains and fluidizes at high strains. (**D**) Stress-strain measurements reveal a shear modulus of 64 Pa and a yield stress of 9 Pa for 0.2% (w/v) Carbopol gel. (**E**) The cross-sectional area of written features exhibits nearly ideal behavior over a wide range of tip speeds, *v*, and flow rates, *Q*. The trend line corresponds to the volume conserving relationship, $Q = \frac{1}{4}\pi abv$.

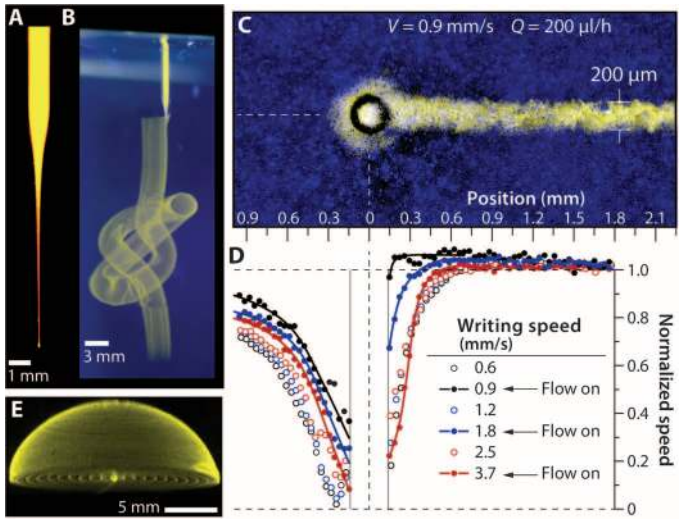

Fig. 2. Stable writing in the granular gel medium. (**A**) Injection tip filled with fluorescent microsphere suspension, imaged under UV illumination. (**B**) The tip revisits the same points in space hundreds of times with intermittent injection to create a continuous knot written with aqueous fluorescent microsphere suspension in aqueous granular gel (UV illumination, side and top views). (**C**) Writing structures atop a fluorescence microscope during live imaging allows a detailed study of yielding length scales and time scales. (**D**) The granular gel flow speed along the axis of translation is plotted normalized by the translation speed. Disturbances in flow decay within less than one tip diameter (see fig. S2). (**E**) A hemispherical cap made from uncrosslinked 1-μm microspheres, created 6 months before photographing, exhibits long-term stability provided by the granular gel medium.

in locations that have been previously sheared by the shaft of the writing needle hundreds to thousands of times (fig. S6A and Fig. 2A). Such a structure cannot be produced with established methods involving crevasses and filler fluids. The additional ability to stop writing in any location, write structures elsewhere, and return to the original location enabled us to create a left-handed overhand knot. This structure cannot be created with extant 3D printing methods without simultaneously building a support structure, even if crosslinking is performed during the printing process (*22*). The stability provided by the granular gel medium allows for unconnected parts of the knot to be created independently and joined later (movie S3). Uncrosslinked structures were also found to be incredibly stable in time, with the oldest retained model exhibiting no visible changes over more than 6 months (Fig. 2, B and E). The stability of the granular gel medium can be further illustrated by considering a limiting case; a gold sphere with a diameter of 400 μm will not sink in a granular gel with a middle-ranged yield stress of 50 Pa.

The soft granular gel permits repeated retracing of the writing needle because the jamming/unjamming transition occurs locally and without a change in composition or material properties. The time scale of this transition is often called the thixotropic time; granular gels such as Carbopol are nonthixotropic or "ideal" because they rapidly achieve steady material properties after abrupt changes in applied shear stress (*3*). We measured the role of thixotropy in the writing process by mounting an injection system on an inverted fluorescence microscope and imaging fluorescent microparticles embedded in the granular gel. PIV (particle image velocimetry) analysis of high-speed video revealed that the flow of granular gel is only disturbed in the immediate vicinity of the writing tip, limited to a range of about one tip diameter. Analysis of the velocity fields at different translation speeds with and without flowing material from the injecting tip showed that the thixotropy time scale is insensitive to tip translation speed. Moreover, the thixotropy time scale and length scale were improved by flowing material from the tip during translation, accelerating the solidification process behind the moving tip. This ideal thixotropic behavior ensures that written structures are trapped into place immediately after being placed into the granular gel, facilitating control and precision (Fig. 2, C and D, and fig. S2).

Polymeric structures are of growing interest for their potential use in medicine and flexible electronics (*21*). Mixtures of polymers and colloids were written into the granular gel medium; mesh structures made from polyvinyl alcohol (PVA) in aqueous granular gel and polydimethylsiloxane (PDMS) in oil-based granular gel showed excellent stability in their solvent-matched medium. The uncrosslinked mesh structures were imaged with confocal fluorescence microscopy and revealed no systematic reduction in surface curvature or feature shape with repeated measurements over several hours (fig. S6B). In principle, writing in the granular gel medium provides precision and stability that is not dominated by the rheological behavior of the writing medium. As evidence of this quality, we produced a set of closed-shell structures made from PVA, polyacrylamide, polyethylene glycol, hyaluronic acid, and sodium alginate, which have viscous moduli spanning a range of an order of magnitude above and below the characteristic yield stress of the granular gel (fig. S7). This level of stability and precision gained from writing

in the granular gel medium enabled the straightforward production and removal of complex precise structures by crosslinking the polymer after writing.

Condensed anisotropic particles assemble and move in elaborate patterns and are integral to the study of complex self-assembling materials (*23*–*25*). We created anisotropic particles in the granular gel medium by writing arrays of high aspect ratio, 400-μm-diameter chiral rods made from photocrosslinkable PVA and fluorescent microspheres. The PVA hydrogel was photocrosslinked in the transparent granular gel, and after removing the helical rods from the granular gel, they showed a high degree of flexibility when allowed to freely move and assemble in a water bath. At high packing density, the soft rods locally align from steric interactions and frequently bend with hairpin turns. The low elastic modulus required for such bends to occur was characterized with indentation measurements on individual rods. We found an elastic modulus of about 2 kPa, which is comparable to the elasticity of several types of soft, living cells (*26*, *27*). Writing in the granular gel medium immediately enables the rapid and precise fabrication of soft, athermal particles over a seemingly unlimited range of size, shape, and form (fig. S6, C and D, and movie S4).

Freestanding objects with microscopic structural detail are challenging to produce with soft delicate materials such as hydrogels. We have created several complex multiscale structures in the granular gel medium made of crosslinked PVA hydrogels and fluorescent colloids. A simple geometric model of an octopus was made with eight tilted and tapering helical shells that mimic tentacles and a bulbous shell as the body. Each tentacle was drawn in a single pass by following surface coordinates along a helical path. The tightly coiled helices had a 100-μm vertical pitch and line widths about 100 μm in diameter. The structure was stable during writing and exhibited no visible changes after ultraviolet (UV) crosslinking. Crosslinking was performed about 6 hours after starting the writing process, demonstrating extremely long working times achievable with this method. The octopus was removed from the granular gel by immersion into a gently agitated water bath. After the granular gel dispersed, the octopus showed strength and integrity while freely fluctuating in the convective currents (Fig. 3, A to C, and movie S5). A similar model of a jellyfish with solid tentacles was created by increasing the volumetric injection rate during writing, and it too exhibited lifelike motion (frequently inverting and entangling) in the water bath after removal from the granular gel (Fig. 3, D and E, and movie S6).

Material encapsulation is a challenging technological task, and huge advancements may be made by controllably generating capsular 3D cocultures of multiple cell types, multispecies microbial colonies, diffusively communicating chemical reaction vessels, smart materials with breakable shells for controlled release, or nested conductors for capacitance sensing (*28*–*31*). Closed shells can be easily manufactured in the granular gel medium, and complex nested structures made from multiplexed arrays of nozzles and materials can be envisioned. To demonstrate the feasibility and ease of encapsulation, we created a miniature assembly of nested Russian dolls. Four closed-shell structures were created, with each larger doll containing all of the others inside; the final assembly reveals nearly seamless joining of individual dolls and illustrates the level of control provided by writing in granular gels (Fig. 3F).

The ability to create living tissue on demand is a major goal in bioengineering, but fluid transport for oxygen and metabolite exchange remains one of the greatest impediments to making macroscopic structures from living cells (*32*). The metabolic needs of cells require a dense vasculature, and cell aggregates larger than a few hundred micrometers cannot survive without such a transport system. Living tissues circumvent this challenge by being packed with interfaces, manifolds, and blood vessels, often found within only a few hundred micrometers from any point in space. To begin to create and study structures as intricate and delicate as living tissue, it is imperative to controllably produce branched tubular networks. We designed and manufactured a complex tubular network

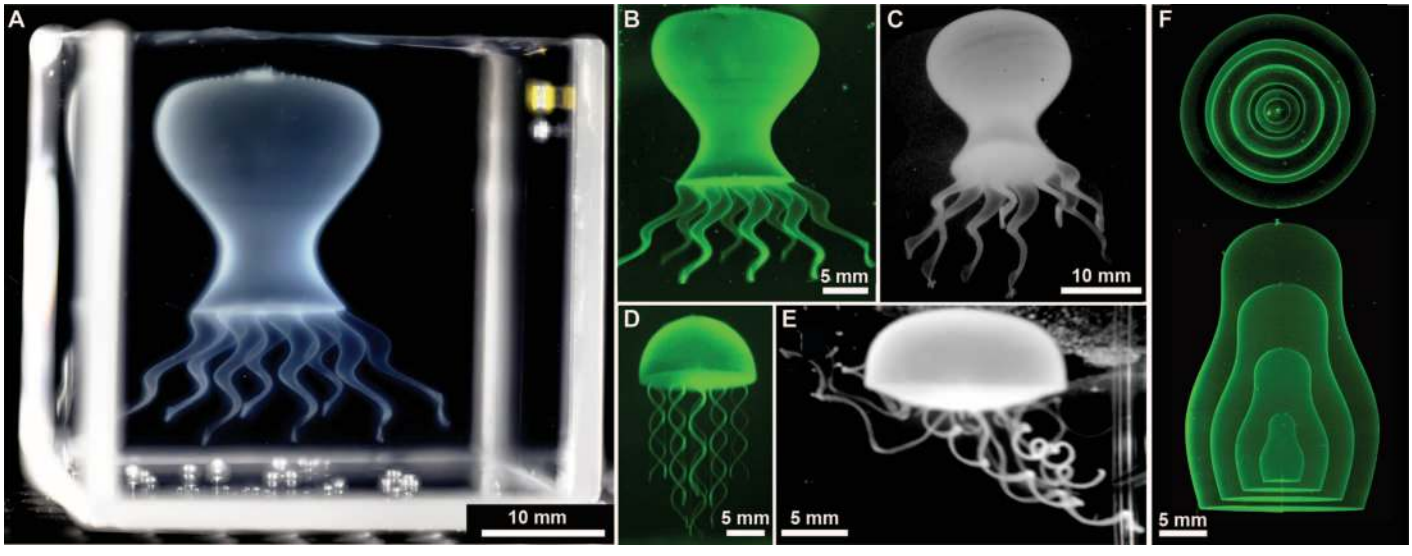

Fig. 3. Writing solid shells and capsules. (**A**) A thin-shell model octopus is made from multiple connected hydrogel parts with a complex, stable surface before polymerization. (**B**) A fluorescence image of the octopus model after polymerization, still trapped in granular gel, exhibits no structural changes from the polymerization process. (**C**) The polymerized octopus model retains integrity after removal from the granular gel, shown floating in water. (**D**) A model jellyfish incorporates flexible high aspect ratio tentacles attached to a closed-shell body. (**E**) Freely floating in water, the jellyfish model exhibits robustness and flexibility. (**F**) Model Russian dolls demonstrate the ability to encapsulate with nested thin shells. Photographs in (A), (C), and (E) were illuminated with white light, and those in (B), (D), and (F) were illuminated with UV light, shown with false-color look-up table (LUT) to enhance weak features.

composed of tapered pipes connected by smoothly morphing quaternary intersections, which have both convex and concave curvatures. The structure is written from a single 25-mm-diameter circular base and has three levels of division, ultimately ending with 27 narrow capillaries that taper to about 100 μm in diameter; the entire structure contains 40 connected vessels and 12 junctions. This network of tubes was made from a biocompatible PVA formulation used in contact lens manufacturing, known by the United States Adopted Name nelfilcon A. The wall thickness of these tubes is about 100 μm, which is thin enough to image single traces along the writing path when examined under high magnification (Fig. 4, A to D). The same striations are observed in the octopus and jellyfish models mentioned earlier, demonstrating that a continuous structure at the limit of feature separation can be achieved by matching the feature width to the helical pitch. By increasing the injection rate during writing, a thicker (~200-μm wall thickness) and more robust structure was made and removed from the granular gel. When placed in a water bath, it can be seen to bend and undulate as water flows past its numerous branches (Fig. 4E and movies S7 and S8).

It is possible to both write and grow living tissue cells in a granular gel culture medium, which is prepared by using cell growth media as a solvent. Observations of cell migration and division demonstrate the potential of the granular gel as a suitable medium for 3D cell culture (movie S9). We have made vascular networks written entirely out of human aortic endothelial cells (HAECs), without the PVA matrix, but the resulting structures are invisible to the naked eye because the refractive index of cells is so closely matched with water and the printed structures are so thin. We used fluorescence confocal microscopy to image a portion of a junction assembly by writing the structure within the microscope's working distance. Projections and slices from the stack show a tilted hollow tube with ~300-μm-thick walls made from HAECs (fig. S8A). The shape matches a corresponding structure that was made from polymers and colloids and has an average variation in thickness on the order of a single cell. Thin flat layers of Madin-Darby canine kidney (MDCK) cells were made with a similar protocol while simultaneously writing collagen through a second injection tip in parallel (fig. S8B). To test the potential limits of precision when writing with cells in the granular gel medium, long lines of MCF10A epithelial cells were written at varying tip speeds, and single cell width features were achieved (fig. S8C). Epithelial and endothelial tissues throughout the body are composed of layers just one cell thick; medical fabrication that faithfully follows biological design requires positioning and control at the length scale of a single cell.

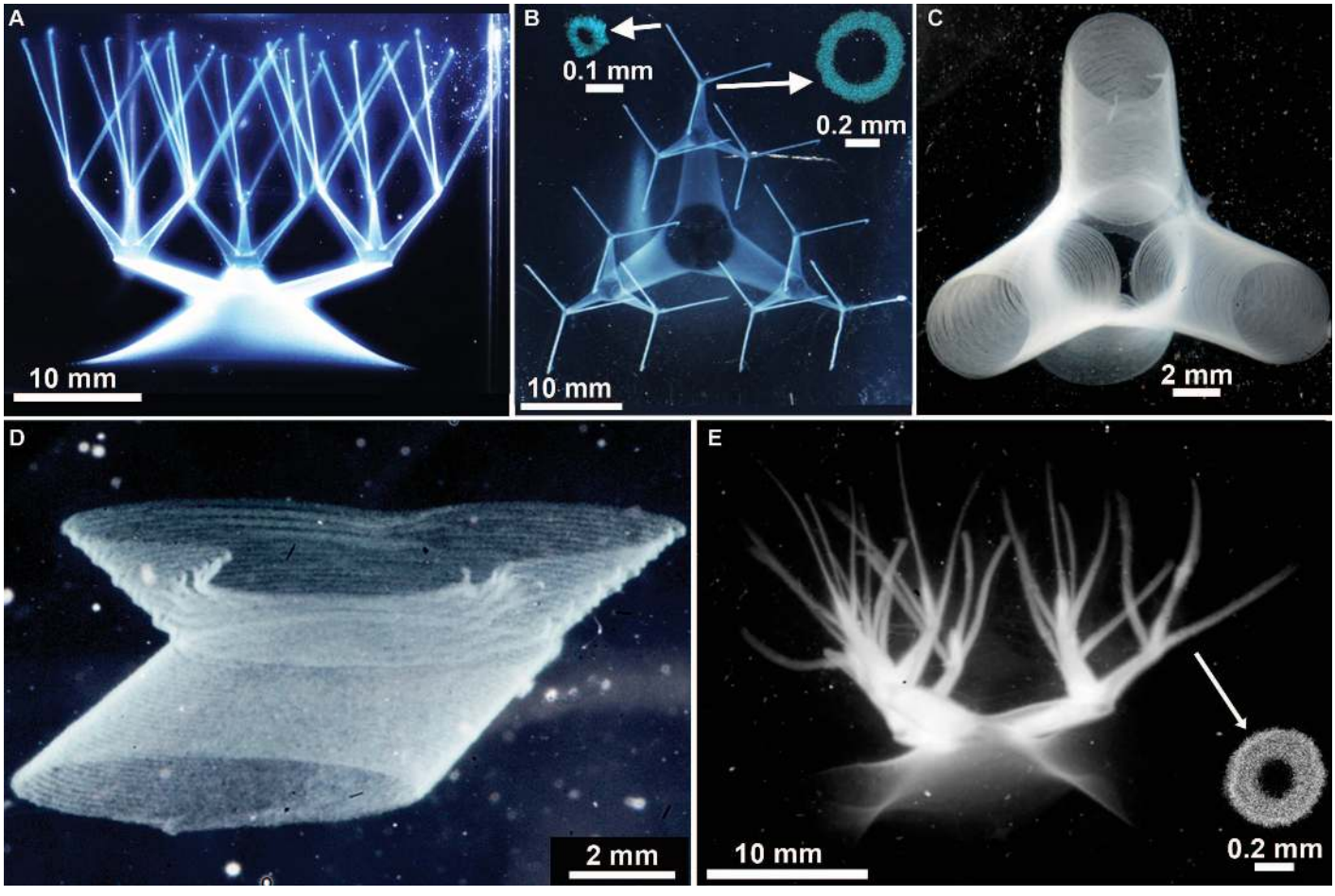

Fig. 4. Hierarchically branched tubular networks. (**A** and **B**) A continuous network of hollow vessels with features spanning several orders of magnitude in diameter and aspect ratio (insets: confocal cross sections). (**C**) A high-resolution photo of truncated vessels around a junction shows hollow tubes with thin walls and features about 100 μm in diameter. (**D**) Junctions exhibit stable concave and convex curvatures. (**E**) A crosslinked network, removed from the granular gel, photographed freely floating in water (inset: confocal cross section).

The limits on size, speed, precision, and materials have yet to be fully defined for writing structures in granular gels (fig. S4). However, this simple medium removes numerous technical barriers to the creation of finely detailed multidimensional structures by using the graceful behavior across the yield point to trap and hold delicate features within a jammed gel made from soft, athermal particles. The remarkable properties of the soft granular gel medium provide stability and versatility within an easy framework that can be immediately integrated into existing platforms across numerous areas from flexible electronics to biology and medicine.

MATERIALS AND METHODS

Granular gel medium preparation

To prepare the soft granular gel medium, 0.2% (w/v) Carbopol ETD 2020 polymer (Lubrizol Co.) is suspended in ultrapure water (18.2 megohms-cm) and 0.01 N NaOH. The various available formulations of Carbopol swell to a differing extent at different pH values. Carbopol ETD 2020 swells maximally at physiological pH values, making it suitable for cell culture applications. For writing with photocrosslinkable polymer solution, 0.05% (w/v) Irgacure photoinitiator (Sigma-Aldrich) is mixed with the Carbopol granular gel. When writing with cells, the gel medium is prepared with cell growth media. Powdered Carbopol (0.7%, w/v) is dispersed into cell growth media at 37°C under sterile conditions, and the gel medium is incubated at 37°C and 5% CO_2 for 24 hours before writing. Other Carbopol concentrations have been explored (0.05 to 1%), as described in the Supplementary Materials. For writing PDMS structures, Dow Corning 9041 silicone elastomer blend is diluted by 10% (w/w) with silicone oil and is used as the granular gel medium. All types of gel medium are homogenized by mixing at 3000 rpm in a speed mixer followed by centrifugation to remove gas bubbles.

Writing medium preparation

Fluorescent polystyrene microspheres (Thermo Scientific) 1 μm in diameter are prepared at a concentration of 0.1% (w/v) for writing, making the writing medium fluorescent and turbid. When writing water-based polymer structures, the microspheres are dispersed in an aqueous solution of photocrosslinkable polyvinyl alcohol (nelfilcon A, provided by Alcon Laboratories). After mixing, the polymer concentration is about 27% (w/v) and the microsphere concentration is 0.1% (w/w). Sylgard 184 (Dow Corning) is used for writing PDMS structures. The PDMS elastomer base is mixed with curing agent at a 10:1 weight ratio. To disperse fluorospheres in the PDMS, a solvent exchange from water to methanol is performed. A concentrated drop of methanol-microsphere suspension is homogeneously dispersed in PDMS with a speed mixer at a final concentration of about 0.1% (w/v). Structures printed with photocrosslinkable PVA are cured with a 100 mW/cm^2 UV lamp. The Carbopol gel medium is washed with water to remove the cured structure.

Writing in the granular gel medium

The 3D writing instrument is composed of a syringe pump for injecting material into the granular gel and three linear translation stages (M-403.2DG from Physik Instrumente) that provide relative motion to the injection tip. Injection tips with an inner diameter of 50 μm are made out of glass microcapillaries (1-mm inner diameter) using a pipette puller (David Kopf Instruments). While printing cells, injection tips of 200-μm inner diameter are used. To reduce wetting of written material to the injection tip, the glass tips are given a hydrophobic surface coating of triethoxy (octyl) silane for printing water-based polymer solution and a hydrophilic surface coating of (3-aminopropyl) triethoxysilane for printing PDMS structures. The syringe pump and the stages are coupled together and programed with MATLAB to inject the writing material at the chosen flow rate while tracing out a path in space. Surface coordinates of structures are generated from analytical 3D functions in the form of closely packed helices. The tangential speed of the microcapillary is kept constant while writing into the granular gel medium.

Cell culture for writing in the granular gel medium

HAECs are cultured in EBM-2 (endothelial cell basal medium-2) supplemented with 2% fetal bovine serum and vascular endothelial growth factor (Lonza). MDCK cells are cultured in high-glucose Dulbecco's modified Eagle's medium (DMEM) supplemented with 5% fetal bovine serum and 1% penicillin-streptomycin. MCF10A cells are cultured in mammary epithelial growth medium (Lonza). Cells are incubated at 37°C in 5% CO_2 and grown to confluence in six-well plates. Cells are fluorescently dyed by treating with 2 μM 5-chloromethylfluorescein diacetate (CMFDA) in serum-free medium and 0.15% dimethyl sulfoxide for 30 min. After dyeing, cells are immediately washed with phosphate buffer saline, trypsinized, and harvested. About 10^6 cells are then concentrated loaded into a syringe. The writing process is performed under sterile conditions at 37°C. For writing collagen in parallel to MDCK cell writing, bovine collagen monomer is kept cold and under acidic conditions until it is deposited into the warm, pH-neutral granular gel medium. This is achieved by pumping the collagen with a separate syringe pump and merging the two writing needles at the point of injection. Cell viability in the granular gel medium is tested by dyeing cell structures in 2 μM calcein-AM and imaging with confocal microscopy after about 1 hour.

Photography and microscopy

Photographs are taken using a Nikon D3X camera under bright-field and UV illumination. Videos are recorded using a Nikon 3100 camera or an Imaging Source DMK 21AU04 camera under white light illumination. Micrographs are taken with a Nikon Eclipse Ti-E microscope with a C2 confocal scanning system. All image and video processing is done using ImageJ.

SUPPLEMENTARY MATERIALS

Supplementary material for this article is available at http://advances.sciencemag.org/cgi/content/full/1/8/e1500655/DC1

Materials and Methods
Fig. S1. Granule size.
Fig. S2. Microscopic imaging of writing in the granular gel medium.
Fig. S3. Tip speed, injection rate, and feature width.
Fig. S4. Scaling and limits of feature width.
Fig. S5. Rheological characterization of the granular gel medium.
Fig. S6. Stable writing in the granular gel medium.
Fig. S7. Writing with rheologically disparate materials.
Fig. S8. Writing with living cells.
Movie S1. Microscopic imaging of writing in the granular gel medium.
Movie S2. Writing nested Russian dolls in the granular gel medium.
Movie S3. Writing a knot in the granular gel medium.
Movie S4. Chiral rod array written in the granular gel medium.
Movie S5. Model octopus shell structure.
Movie S6. Model jellyfish structure with flexible, solid tentacles.
Movie S7. Hierarchically branching tubular network.
Movie S8. Freely floating branched network.
Movie S9. Cell migration and division in the granular gel medium.

REFERENCES AND NOTES

1. J. Mattsson, H. M. Wyss, A. Fernandez-Nieves, K. Miyazaki, Z. Hu, D. R. Reichman, D. A. Weitz, Soft colloids make strong glasses. *Nature* **462**, 83–86 (2009).
2. B. R. Saunders, B. Vincent, Microgel particles as model colloids: Theory, properties and applications. *Adv. Colloid Interface Sci.* **80**, 1–25 (1999).
3. C. J. Dimitriou, R. H. Ewoldt, G. H. McKinley, Describing and prescribing the constitutive response of yield stress fluids using large amplitude oscillatory shear stress (LAOStress). *J. Rheol.* **57**, 27–70 (2013).
4. C. S. O'Hern, L. E. Silbert, A. J. Liu, S. R. Nagel, Jamming at zero temperature and zero applied stress: The epitome of disorder. *Phys. Rev. E* **68**, 011306 (2003).
5. A. J. Liu, S. R. Nagel, Nonlinear dynamics: Jamming is not just cool any more. *Nature* **396**, 21–22 (1998).
6. M. E. Cates, J. P. Wittmer, J.-P. Bouchaud, P. Claudin, Jamming, force chains, and fragile matter. *Phys. Rev. Lett.* **81**, 1841 (1998).
7. A. J. Liu, S. R. Nagel, *Jamming and Rheology: Constrained Dynamics on Microscopic and Macroscopic Scales* (CRC Press, Boca Raton, FL, 2001).
8. D. Bi, J. Zhang, B. Chakraborty, R. P. Behringer, Jamming by shear. *Nature* **480**, 355–358 (2011).
9. E. I. Corwin, H. M. Jaeger, S. R. Nagel, Structural signature of jamming in granular media. *Nature* **435**, 1075–1078 (2005).
10. P. Menut, S. Seiffert, J. Sprakel, D. A. Weitz, Does size matter? Elasticity of compressed suspensions of colloidal- and granular-scale microgels. *Soft Matter* **8**, 156–164 (2012).
11. K. S. Schweizer, G. Yatsenko, Collisions, caging, thermodynamics, and jamming in the barrier hopping theory of glassy hard sphere fluids. *J. Chem. Phys.* **127**, 164505 (2007).
12. E. C. Cho, J.-W. Kim, A. Fernández-Nieves, D. A. Weitz, Highly responsive hydrogel scaffolds formed by three-dimensional organization of microgel nanoparticles. *Nano Lett.* **8**, 168–172 (2008).
13. A. Fernandez-Nieves, H. Wyss, J. Mattsson, D. A. Weitz, *Microgel Suspensions: Fundamentals and Applications* (Wiley, 2011), p. 500.
14. J. D. Debord, S. Eustis, S. Byul Debord, M. T. Lofye, L. A. Lyon, Color-tunable colloidal crystals from soft hydrogel nanoparticles. *Adv. Mater.* **14**, 658–662 (2002).
15. E. J. Banigan, M. K. Illich, D. J. Stace-Naughton, D. A. Egolf, The chaotic dynamics of jamming. *Nat. Phys.* **9**, 288–292 (2013).
16. G. M. Gratson, M. Xu, J. A. Lewis, Microperiodic structures: Direct writing of three-dimensional webs. *Nature* **428**, 386 (2004).
17. J. Stringer, B. Derby, Formation and stability of lines produced by inkjet printing. *Langmuir* **26**, 10365–10372 (2010).
18. B. Y. Ahn, E. B. Duoss, M. J. Motala, X. Guo, S.-I. Park, Y. Xiong, J. Yoon, R. G. Nuzzo, J. A. Rogers, J. A. Lewis, Omnidirectional printing of flexible, stretchable, and spanning silver microelectrodes. *Science* **323**, 1590–1593 (2009).
19. S. V. Murphy, A. Atala, 3D bioprinting of tissues and organs. *Nat. Biotechnol.* **32**, 773–785 (2014).
20. W. Wu, A. DeConinck, J. A. Lewis, Omnidirectional printing of 3D microvascular networks. *Adv. Mater.* **23**, H178–H183 (2011).
21. J. T. Muth, D. M. Vogt, R. L. Truby, Y. Mengüç, D. B. Kolesky, R. J. Wood, J. A. Lewis, Embedded 3D printing of strain sensors within highly stretchable elastomers. *Adv. Mater.* **26**, 6307–6312 (2014).
22. J. R. Tumbleston, D. Shirvanyants, N. Ermoshkin, R. Janusziewicz, A. R. Johnson, D. Kelly, K. Chen, R. Pinschmidt, J. P. Rolland, A. Ermoshkin, E. T. Samulski, J. M. DeSimone, Continuous liquid interface production of 3D objects. *Science* **347**, 1349–1352 (2015).
23. S. C. Glotzer, M. J. Solomon, Anisotropy of building blocks and their assembly into complex structures. *Nat. Mater.* **6**, 557–562 (2007).
24. V. Narayan, S. Ramaswamy, N. Menon, Long-lived giant number fluctuations in a swarming granular nematic. *Science* **317**, 105–108 (2007).
25. X.-q. Shi, Y.-q. Ma, Topological structure dynamics revealing collective evolution in active nematics. *Nat. Commun.* **4**, 3013 (2013).
26. N. Wang, I. M. Tolić-Nørrelykke, J. Chen, S. M. Mijailovich, J. P. Butler, J. J. Fredberg, D. Stamenović, Cell prestress. I. Stiffness and prestress are closely associated in adherent contractile cells. *Am. J. Physiol. Cell Physiol.* **282**, C606–C616 (2002).
27. D. E. Discher, P. Janmey, Y.-l. Wang, Tissue cells feel and respond to the stiffness of their substrate. *Science* **310**, 1139–1143 (2005).
28. A. S. Utada, E. Lorenceau, D. R. Link, P. D. Kaplan, H. A. Stone, D. A. Weitz, Monodisperse double emulsions generated from a microcapillary device. *Science* **308**, 537–541 (2005).
29. S.-Y. Teh, R. Lin, L.-H. Hung, A. P. Lee, Droplet microfluidics. *Lab Chip* **8**, 198–220 (2008).
30. N. Tompkins, N. Li, C. Girabawe, M. Heymann, G. B. Ermentrout, I. R. Epstein, S. Fradena, Testing Turing's theory of morphogenesis in chemical cells. *Proc. Natl. Acad. Sci. U.S.A.* **111**, 4397–4402 (2014).
31. J. Zhang, R. J. Coulston, S. T. Jones, J. Geng, O. A. Scherman, C. Abell, One-step fabrication of supramolecular microcapsules from microfluidic droplets. *Science* **335**, 690–694 (2012).
32. J. S. Miller, K. R. Stevens, M. T. Yang, B. M. Baker, D.-H. T. Nguyen, D. M. Cohen, E. Toro, A. A. Chen, P. A. Galie, X. Yu, R. Chaturvedi, S. N. Bhatia, C. S. Chen, Rapid casting of patterned vascular networks for perfusable engineered three-dimensional tissues. *Nat. Mater.* **11**, 768–774 (2012).

Acknowledgments: We thank A. Fernandez-Nieves and Y.-W. Chang for sharing their expertise in granular yield stress materials. We also thank D. Pawson, curator of The Museum of Knots and Sailors' Ropework in Suffolk, UK, for instructions on knot nomenclature. **Funding:** This material is based on work supported by the National Science Foundation under grant no. DMR-1352043. **Author contributions:** T.B., S.J., S.M.Z., and R.M.N. prepared materials; T.B. and S.J. wrote structures into the granular gel medium; K.G.R. constructed the 3D writing system; T.B., K.G.R., and T.E.A. wrote control algorithms and code for generating 3D surface coordinates of written structures; S.M.Z. performed cell culture; T.B., S.J., S.M.Z., R.M.N., and T.E.A. performed microscopy and photography. All authors contributed to data analysis, discussion, and manuscript preparation. **Competing interests:** The authors declare that they have no competing interests. **Data and materials availability:** The data presented here are available upon request (email: t.e.angelini@ufl.edu).

Submitted 21 May 2015
Accepted 4 June 2015
Published 25 September 2015
10.1126/sciadv.1500655

Citation: T. Bhattacharjee, S. M. Zehnder, K. G. Rowe, S. Jain, R. M. Nixon, W. G. Sawyer, T. E. Angelini, Writing in the granular gel medium. *Sci. Adv.* **1**, e1500655 (2015).

ScienceAdvances
AAAS

Writing in the granular gel medium

Tapomoy Bhattacharjee, Steven M. Zehnder, Kyle G. Rowe, Suhani Jain, Ryan M. Nixon, W. Gregory Sawyer and Thomas E. Angelini (September 25, 2015)

Sci Adv 2015, 1:.
doi: 10.1126/sciadv.1500655

Science Advances

AAAS

advances.sciencemag.org/cgi/content/full/1/8/e1500655/DC1

Supplementary Materials for

Writing in the granular gel medium

Tapomoy Bhattacharjee, Steven M. Zehnder, Kyle G. Rowe, Suhani Jain, Ryan M. Nixon, W. Gregory Sawyer, Thomas E. Angelini

Published 25 September 2015, *Sci. Adv.* **1**, e1500655 (2015)
DOI: 10.1126/sciadv.1500655

The PDF file includes:

Other Supplementary Material for this manuscript includes the following:
(available at advances.sciencemag.org/cgi/content/full/1/8/e1500655/DC1)

Movie S1 (.mov format). Microscopic imaging of writing in the granular gel medium.
Movie S2 (.mov format). Writing nested Russian dolls in the granular gel medium.
Movie S3 (.mov format). Writing a knot in the granular gel medium.
Movie S4 (.mov format). Chiral rod array written in the granular gel medium.
Movie S5 (.mov format). Model octopus shell structure.
Movie S6 (.mov format). Model jellyfish structure with flexible, solid tentacles.
Movie S7 (.mov format). Hierarchically branching tubular network.
Movie S8 (.mov format). Freely floating branched network.
Movie S9 (.mov format). Cell migration and division in the granular gel medium.

Supplementary Materials:

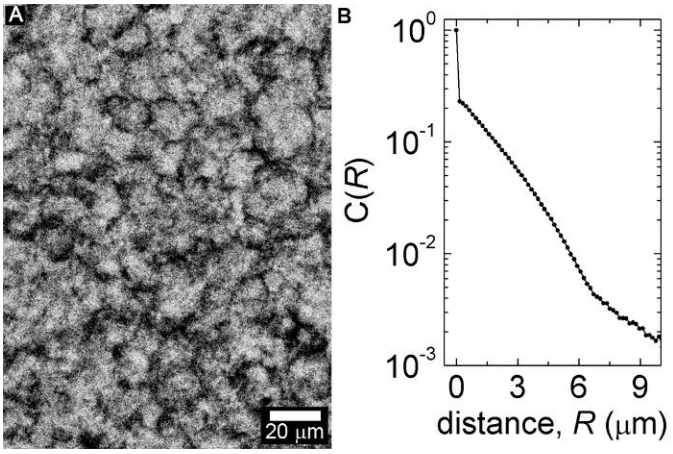

Fig. S1. Granule size. (**A**) Confocal microscopy cross-section of granular gel in which the granules were previously swelled and filled with 20nm fluorospheres, then concentrated again to 0.2% (w/v). (**B**) Intensity-intensity autocorrelation function shows a broad shoulder with a kink at 7μm, indicating the approximate particle size.

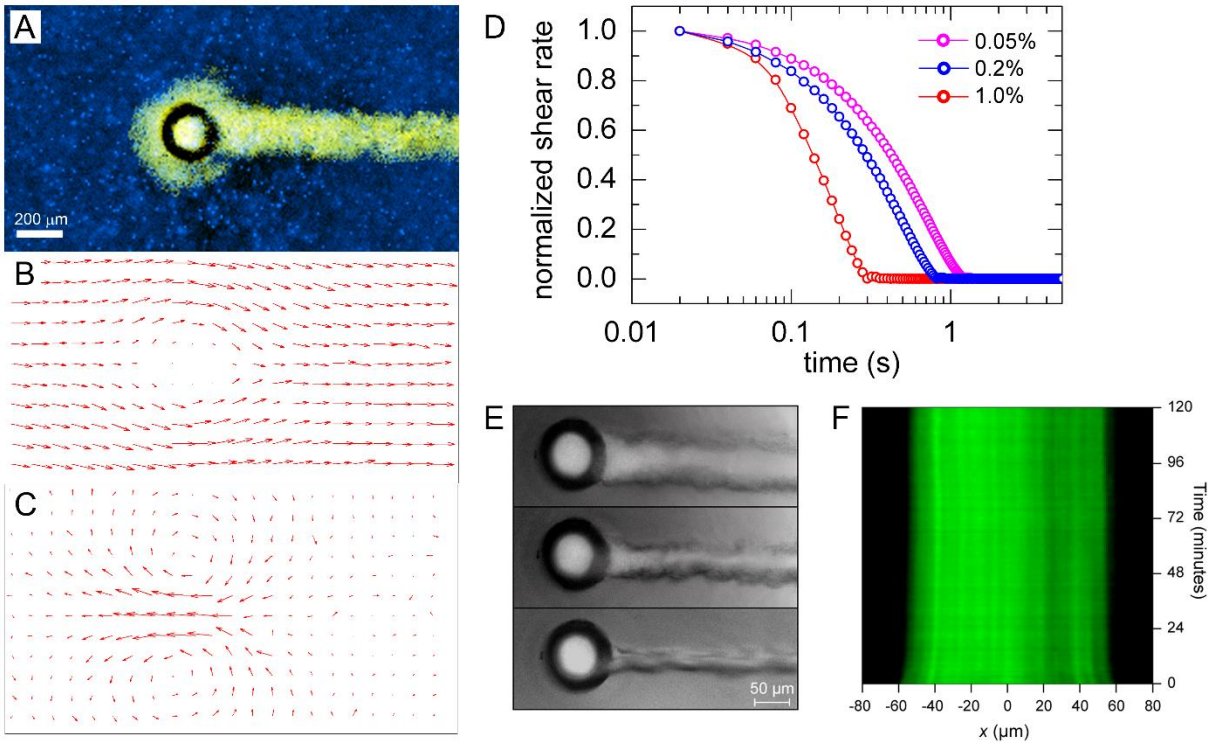

Fig. S2. Microscopic imaging of writing in the granular gel medium. (**A**) We measure the flow field around a translating injection nozzle by writing into the granular gel medium with an instrument mounted on an inverted microscope. Fluorescent particles are used for imaging the flowing gel (blue) and for imaging the injected material (yellow). (**B**) The granular gel medium is

translated relative to a stationary injecting tip, and a velocity field is measured using PIV. (**C**) We observe the distance over which the nozzle disturbs the granular gel medium by subtracting the average far-field velocity from the full velocity field. Along the axis of motion, this distance is seen to be about the diameter of the injection tip. This disturbance in flow speed along the axis of motion is plotted in Fig. 2D (main text) for a variety of translation and flow conditions, always showing a very short thixotropic length-scale of less than 0.6 mm. A corresponding thixotropic time-scale of 0.3s is estimated from the ratio of this length-scale to the translation speed of around 2mm s^{-1}. (**D**) Rheological measurements of thixotropic time demonstrate the same fast recovery of elasticity. Here, the shear rate is plotted for a constant applied stress, immediately after reducing the stress below the yielding threshold (the three curves correspond to three different gel concentrations). (**E**) The dependence of feature width on translation speed is observed during the writing process. Feature width decreases with increasing tip speed (speed increasing from top to bottom). The written features have a lateral roughness of about 10μm, comparable to the size of one or two granular gel particles. (**D**) Fluorescence images of written lines were collected in time-lapse for two hours immediately after the cessation of writing. A cross-sectional slice of the written feature is shown evolving in time as a kymograph. A short relaxation is observed for the first 10 minutes, during which the granular gel medium squeezes inward against the written feature, making the object slightly thinner. The vertical striations correspond to groups of fluorescent particles remaining in the same location throughout the time-lapse, trapped by the granular gel medium.

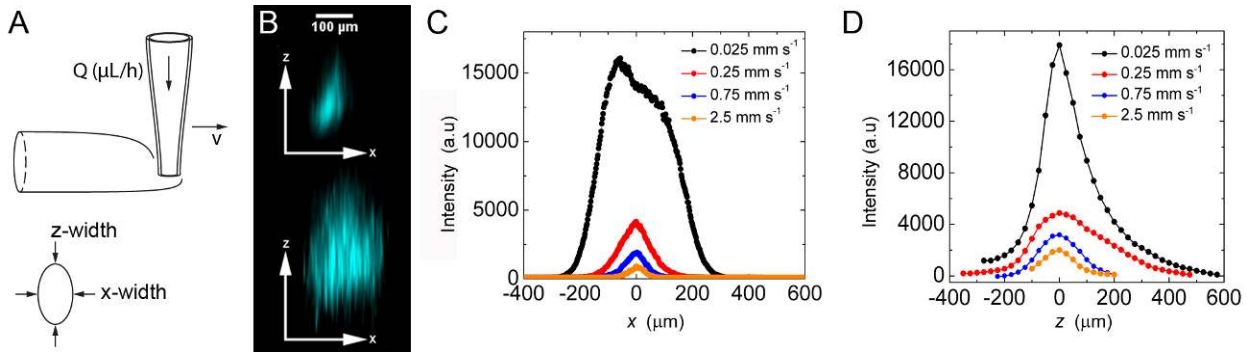

Fig. S3. Tip speed, injection rate, and feature width. (**A,B**) To establish protocols for writing in the granular gel medium, linear features were drawn and measured using different combinations of tip speed, v, and injection rate, Q. Continuous horizontal lines were drawn with tip translation speeds between 0.025 mm s^{-1} and 2.5 mm s^{-1}, and with injection flow rates between 10 μL h^{-1} and 500 μL h^{-1}. A dispersion of 1 μm fluorescent spheres in water was used as the writing medium. To measure the feature size for all combinations of tip speed and injection rate, z-stacks were collected with fluorescence microscopy. A maximum intensity projection in the x-z plane shows a cross-section of a written line (Q = 50 μL h^{-1}, top: v = 2.5 mm s^{-1}, bottom: v = 0.25 mm s^{-1}.). The re-constructed x-z projections were stretched to a true spatial aspect ratio, so features appear stretched along the z direction due to low sampling density of z-slices. (Displayed with a false color LUT to highlight edges). (**C**,**D**) Intensity projections onto the x and z axes are used to quantify the feature sizes along the vertical and lateral writing directions. Example profiles at different tip speeds and Q = 50 μL h^{-1} are shown. Intensity profiles show that feature width along both the x and z directions decrease with increasing tip speed.

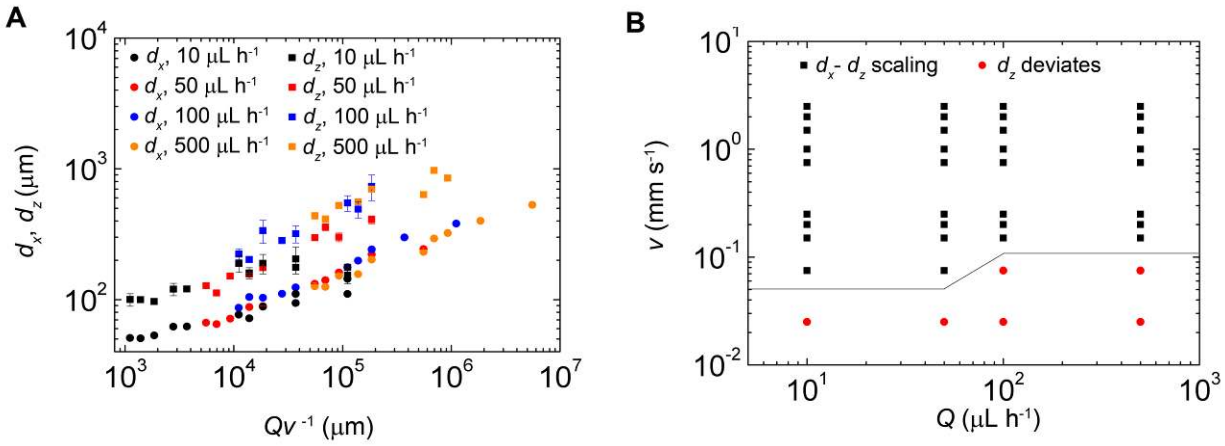

Fig. S4. Scaling and limits of feature width. (**A**) Feature widths d_x and d_z show smooth variation with the injecting tip speed, v over most of the tested range. Error bars are 95% confidence intervals of the full-width at half-maximum parameter in Gaussian functions fit to intensity profiles (no error bar indicates less error than the size of the marker). These trends in feature size versus tip speed systematically increase with increasing injection rate, Q. We plot feature size versus the ratio $Q\ v^{-1}$, finding that the d_x and d_z data lay on universal scaling curves. These data are used to estimate the feature cross-sectional areas, plotted in Fig. 1E (main text). (**B**) From these scaling curves we find that d_z is proportional to d_x over most of the Q-v space explored for writing, allowing the predictable generation of features in both directions. When the tip moves very slowly, however, d_z, deviates and does not scale proportionally with d_x. Here we plot a diagram in Q-v space to identify the boundary between these two regimes of writing in the granular gel medium.

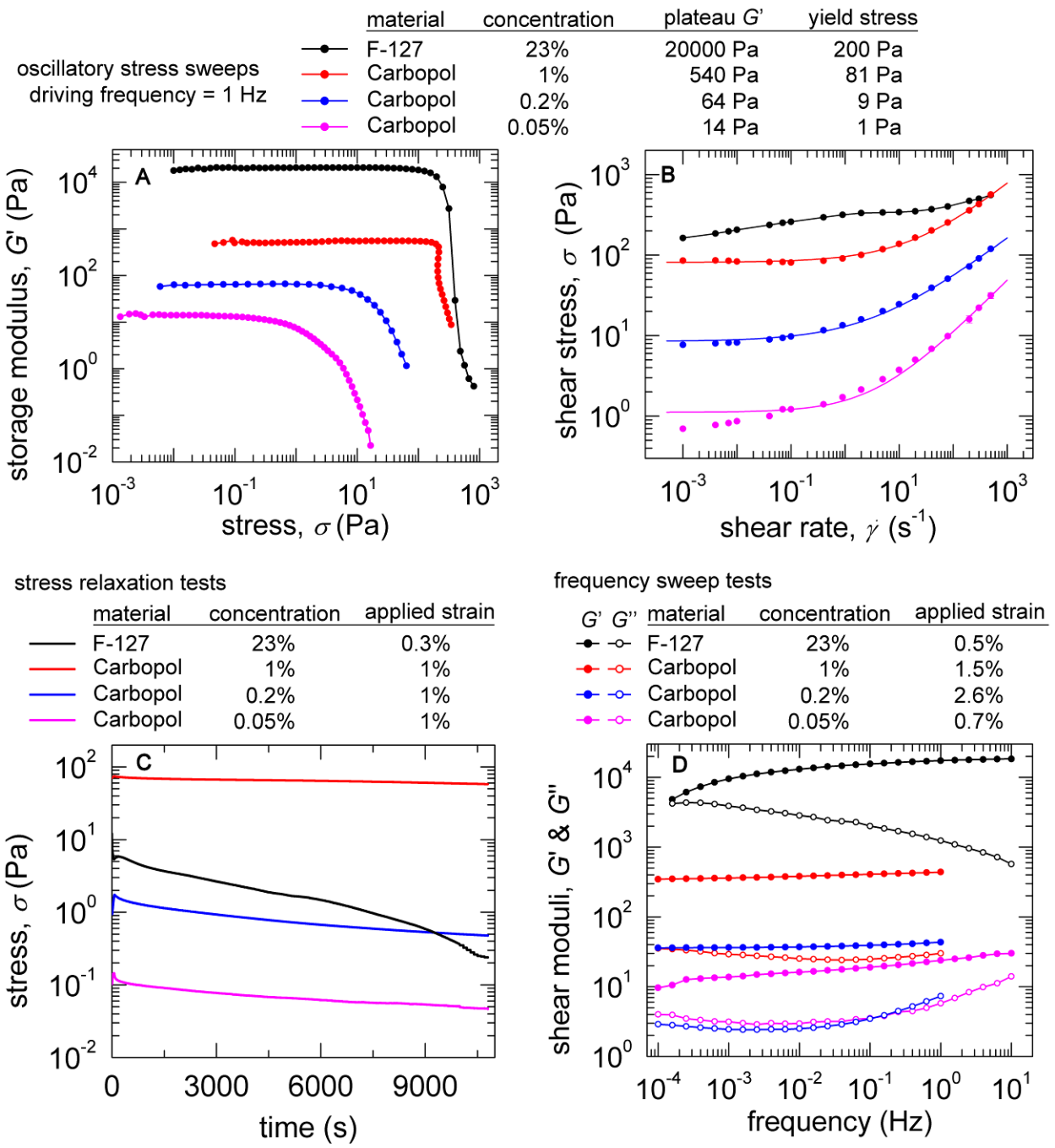

Figure S5. Rheological characterization of the granular gel medium. The granular gel was prepared at three different Carbopol concentrations as described in Methods. To provide a point of comparison, we also prepared samples of F-127 pluronic gel, which has been used previously as an embedding medium for 3D printing. (**A**) Stress-sweeps performed in oscillatory shear were used to measure the low-stress plateau modulus, *G*'. On this logarithmic scale, error bars are less than the size of the data points. (**B**) The drop in modulus at high stress is one indication of yielding. To determine the yield stress quantitatively, a strain-rate sweep is performed, where constant strain rate is maintained and the stress is measured. The measurement is repeated at many strain-rates to generate the curves. The yield stress is found by fitting the data to a classic Herschel-Bulkley

model (see ref. 3). The two higher concentration granular gel samples fit perfectly to the model; the lowest concentration granular gel sample deviates slightly at the lowest strain rates, indicating the presence of some visco-plastic creep at low stresses. By contrast, the f-127 pluronic sample does not behave like a yielding Herschel-Bulkley fluid at these strain rates (spline added to guide the eye). We therefore estimate an effective yield stress for f-127 from the stress at which *G'* deviates from it's plateau value. (**C**) Stress relaxation measurements highlight a major difference between the granular gel and the f-127. At low strains, the granular gels remain stressed over long times, which means that elastic energy is stored in the strained gel, and indicates low levels of microscopic rearrangement. The F-127 showed a persistent reduction in stress throughout the 10^4 second test. This difference may be associated with the granular nature of the gels, versus the thermal nature of the nano-scale micelles comprising the F-127 system. (**D**) To explore the degree of fluid-like behavior in the granular gel medium, frequency sweeps were performed at low applied strains. The granular gel systems all exhibited fairly flat responses, with *G*' and *G*'' remaining separated across the spectrum, behaving almost like a Kelvin-Voigt linear solid with damping. By contrast, the F-127 frequency sweep resembled that of a Maxwell-fluid, suggesting that its solid-like stability is associated with kinetically impeded thermal motion, consistent with its stress-relaxation behavior. These rheological measurements highlight the fundamental properties of soft granular gels that provide great practical versatility for three dimensional writing, enabling the creation of the wide diversity of structures reported here.

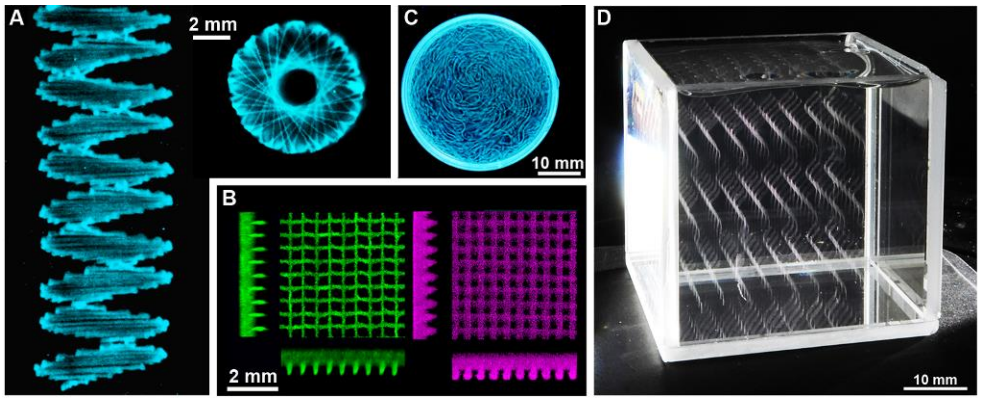

Fig. S6. Stable writing in the granular gel medium. (**A**) The writing tip revisits the same points in space hundreds of times to create a DNA structure written with an aqueous fluorescent microsphere suspension in aqueous granular gel (UV illumination, side and top views). (**B**) Maximum intensity projections (x,y, and z directions) from confocal microscopy z-stacks of PVA mesh (left) and PDMS mesh (right) show uncrosslinked polymer structures stabilized by the granular gel medium. (**C**) Thin rods are written in the granular gel medium, photocrosslinked, removed from the granular gel, and placed in a pertri-dish, where they align and bend. (**D**) These vertical chiral rods hold their shape and orientation with no signs of gravitational effects while in the granular gel.

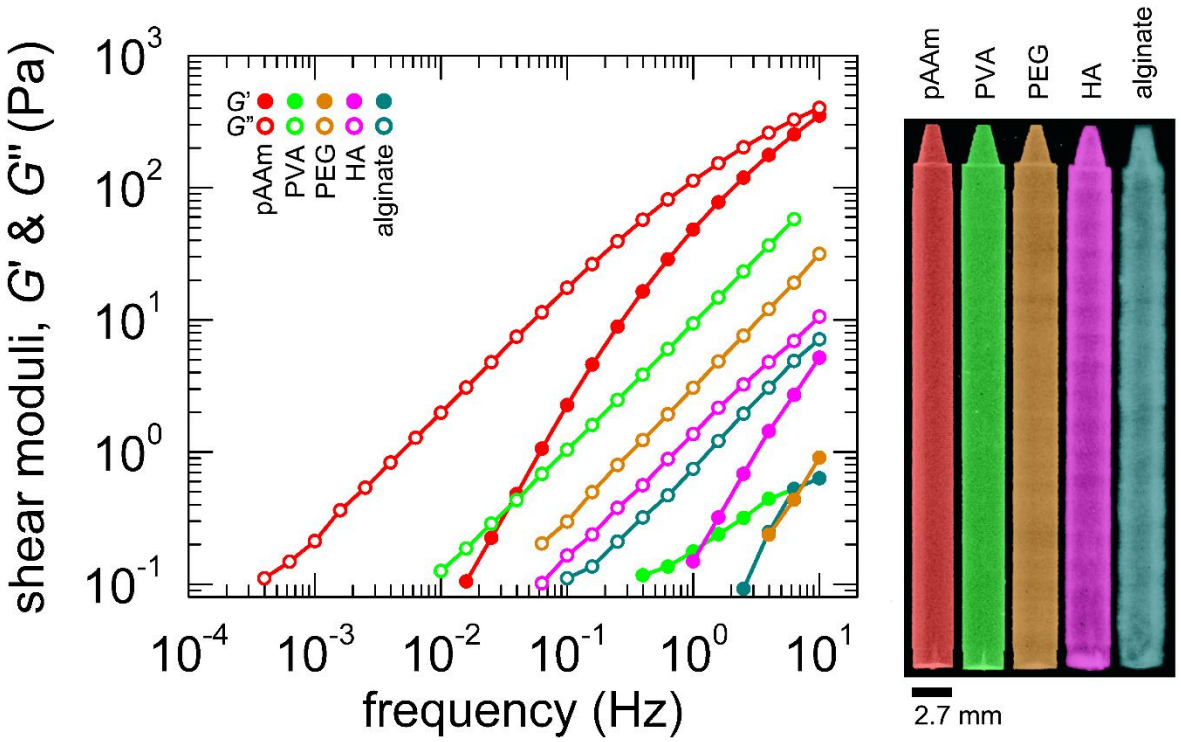

Fig. S7. Writing with rheologically disparate materials. We tested the sensitivity of the granular gel medium to the rheological properties of writing materials by preparing solutions of several polymers at different concentrations and writing the same structure at the same flow rate (10 μL h^{-1}), tip speed (2.5 mm s^{-1}), and granular gel concentration (0.2% w/v). Hollow-shell scale models of crayons 2.78 cm in length (1/3 scale) and approximately 200 μm wall thickness were created from solutions of polyacrylamide (14.3% w/v), PVA (27% w/v), polyethylene glycol (27% w/v), hyaluronic acid (0.95% w/v), and sodium alginate (2.4% w/v). Fluorescent microspheres were added to the polymer solutions to enhance contrast for imaging under a combination of white light and UV illumination. Oscillatory rheological measurements were performed on the polymer solutions at 1% strain. The written polymer materials were found to exhibit widely varying viscoelasticity. For example, at a frequency of 1 Hz, the viscous modulus (G'') of polyacrylamide was found to be 113 Pa, while the viscous modulus of alginate was found to be 0.75 Pa, with the other materials falling between the two. These viscous moduli fall approximately an order of magnitude above and below the yield stress of 0.2% Carbopol, 9 Pa. Writing in the granular gel medium thus provides a broad range of freedom for materials selection without the need for optimization when changing materials, enabling the rapid creation of spatially heterogeneous structures from different materials like tissue-mimicking biomaterials.

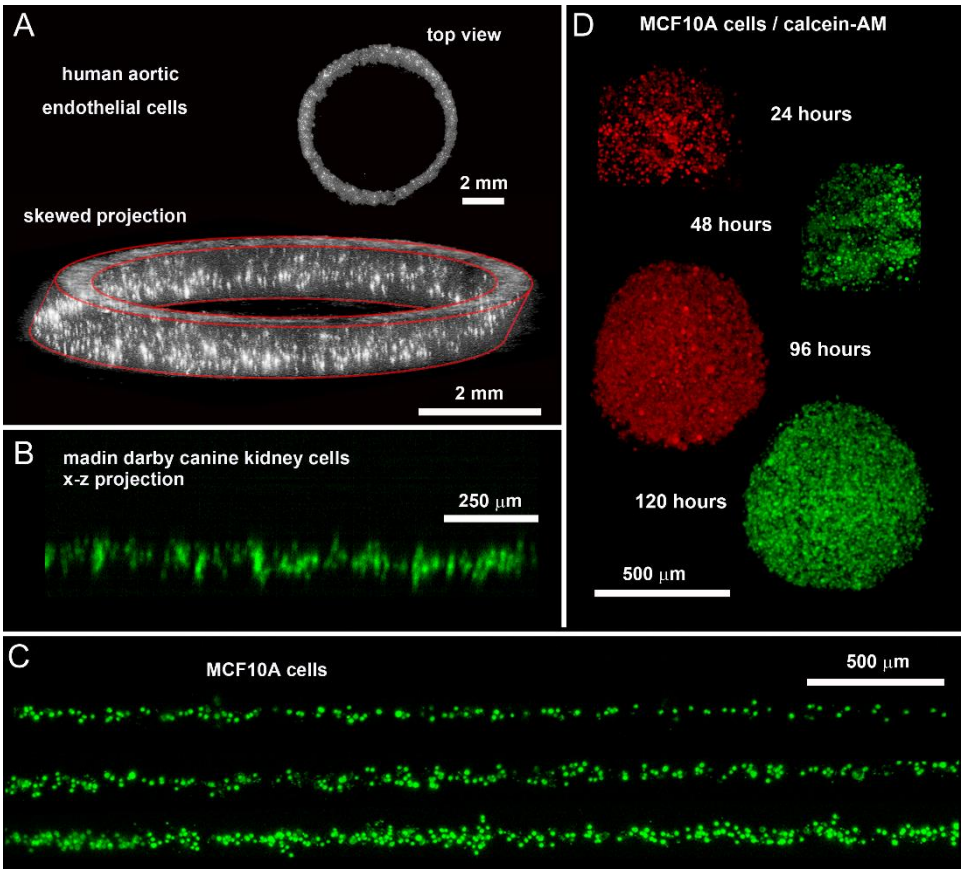

Fig. S8 (**A**) A structure written from only living cells, trapped in granular gel growth media, imaged with confocal fluorescence microscopy. The same tilted tubular structure at the base in Figure 4D is seen here made from fluorescently labelled HAECs. The image is a maximum intensity projection along a skewed direction, and the inset is the XY slice corresponding to the top of the tubular structure. (**B**) Individual cells can be resolved in a flat layer of Madin Darby canine kidney cells written into the granular gel medium. This layer was created by simultaneously writing cells and collagen precursor from two nozzles, fused together. The layer is approximately 100 μm thick, comprising approximately three to five cells in thickness througout the layer. (**C**) Long straight lines of MCF10A epithelial cells were written at varying translation speeds to test the precision achievable while writing with cells. With increasing translation speed, the lines become thinner and thinner (bottom to top) until single cells are injected along the line, one at a time. The cells shown here were dyed with CMFDA prior to writing. (**D**) To check for cell viability, spheroids of MCF10A cells were written into the granular gel. Cells were incubated and monitored over the course of five days. Each day, cells were dyed with calcein-AM and imaged one hour after dyeing. The 24 and 48 hour time points correspond to the same spheroid, where calcein red was used on day one, and calcein green was used on day two. Calcein red and green were used for a different spheroid on day four, and five, respectively.

Movie S1. Microscopic imaging of writing in the granular gel medium. Video fluorescence microscopy of a stationary writing tip injecting a mixture of fluorescent microspheres and PVA polymer into the moving granular gel medium. Translation speed: 0.9 mm s^{-1}. Duration: 5.4 seconds.

Movie S2. Writing nested Russian dolls in the granular gel medium. Time-lapse imaging (bright field) of four nested shell structures modelling miniature Russian dolls. Duration: 4.8 hours.

Movie S3. Writing a knot in the granular gel medium. Time-lapse imaging (bright field) of a left-handed overhand knot. Duration: 54 minutes.

Movie S4. Chiral rod array written in the granular gel medium. Rotating view of vertically oriented chiral rods written inside the granular gel medium.

Movie S5. Model octopus shell structure. Rotating view of a thin shell model octopus written inside the granular gel medium, followed by video of the structure removed from the medium, fluctuating in an agitated water bath.

Movie S6. Model jellyfish structure with flexible, solid tentacles. Thin shell jellyfish model, freely floating in an agitated water bath after being removed from the granular gel medium.

Movie S7. Hierarchical branching tubular network. Rotating view of a hollow vascular network written in the granular gel medium.

Movie S8. Freely floating branched network. Freely floating single branched network structure after being crosslinked and removed from granular gel medium.

Movie S9. Cell migration and division in the granular gel medium. Human aortic endothelial cells were fluorescently dyed with 5-chloromethylfluorescein diacetate, injected into granular gel cell growth medium, and incubated at 37^0C and 5% CO_2. Cells grown in the granular gel medium were seen to divide and migration was observed seven days after seeding.